

See discussions, stats, and author profiles for this publication at: <https://www.researchgate.net/publication/231710829>

Studies on Polymer–Metal Interfaces. 2. Competitive Adsorption between Oxygen- and Nitrogen-Containing Functionality in Model Copolymers onto Metal Surfaces

ARTICLE *in* MACROMOLECULES · MARCH 2000

Impact Factor: 5.8 · DOI: 10.1021/ma982003q

CITATIONS

15

READS

29

2 AUTHORS, INCLUDING:



Dong Ha Kim

Ewha Womans University

136 PUBLICATIONS 3,158 CITATIONS

SEE PROFILE

Studies on Polymer–Metal Interfaces. 2. Competitive Adsorption between Oxygen- and Nitrogen-Containing Functionality in Model Copolymers onto Metal Surfaces

Dong Ha Kim and Won Ho Jo*

Department of Fiber and Polymer Science, Seoul National University, Seoul 151-742, Korea

Received December 28, 1998; Revised Manuscript Received July 26, 1999

ABSTRACT: The competitive adsorption behavior between oxygen- and nitrogen-containing functionality in poly(methyl methacrylate-*co*-2-vinylpyridine) (MMA2VP) and poly(methyl methacrylate-*co*-4-vinylpyridine) (MMA4VP) random copolymers onto alumina substrate was investigated. The adhesive strength of both the MMA2VP/alumina and MMA4VP/alumina systems increased with increasing vinylpyridine (VP) content in the copolymers, and the effect was more prominent for the MMA4VP/alumina system. Analysis of the reflection–absorption infrared spectroscopy shows that the carbonyl functional groups in MMA2VP and MMA4VP interact specifically with alumina while the pyridine rings in VP units are oriented more vertically to alumina surface than carbonyl groups. Results from X-ray photoelectron spectroscopy (XPS) reveal that both the nitrogen-containing functionalities in 2VP or 4VP units and the oxygen-containing functionality in MMA unit interact specifically with alumina surface. The quantitative analysis of XPS spectra indicates that the nitrogen-containing functionality adsorbs more favorably onto alumina surface than the oxygen-containing functionality for both the MMA2VP/alumina and MMA4VP/alumina systems.

Introduction

Adsorption of polymer molecules onto metal surfaces is of major importance in applications such as adhesive bonding, corrosion protection, colloid stabilization, and many other areas.^{1–3} Accordingly, the understanding of the interfacial characteristics between polymer and metal is critical in order to control its chemical and physical properties.

It has been reported that nitrogen-containing polymers can form a complex with metal, which may significantly enhance the adhesive strength between polymer and metal.^{4–6} Among many nitrogen-containing functional groups, the interfacial activity of 2-vinylpyridine (2VP) and 4-vinylpyridine (4VP) on metal surface has extensively been investigated by several workers.^{7–13} Roth and Boerio⁷ studied the adsorption behavior of poly(4-vinylpyridine) (P4VP) onto silver using the surface-enhanced Raman scattering (SERS) technique. They observed the ring breathing mode of the pyridine rings near 1030 cm^{−1}, when the polymer is coated onto silver, and concluded that the pyridine moieties are adsorbed through the nitrogen atoms with a vertical conformation. Xue and co-workers^{8,9} also investigated the surface geometry and orientation of poly(4-vinylpyridine) chains on silver surface by observing the change in the relative intensity of the out-of-plane ring deformation to the in-plane ring stretching vibrational bands in SERS spectra. They found that the pyridine ring lies flat on metal surface with a π -bonded geometry at ambient temperature, whereas the ring stands up to form an N-bonded geometry upon heating. They also observed that different sample doping methods yielded different orientation of polymer chains on the metal surface.

It has also been reported that the interfacial adhesive strength between polymer and metal could be significantly enhanced through metal–oxygen–polymer com-

plex formation when metal atoms were vapor-deposited on oxygen-containing polymers.^{14–16} When the metal films were deposited on an oxygen-containing polymer, X-ray photoelectron spectroscopy (XPS) always detected changes in the photoemission line shapes of carbon and oxygen atoms in the substrate, indicating the formation of metal–oxygen–polymer complex.

In our previous study,¹⁷ we directly compared the effects of the two functionalities (oxygen- vs nitrogen-containing one) on the adhesive strength with metal. For this purpose, poly(styrene-*co*-4-vinylpyridine) (S4VP) and poly(styrene-*co*-acrylic acid) (SAA) were prepared as a representative of polymers with nitrogen- and oxygen-containing functionality, respectively, and the interfacial activity of these polymers onto metal surface was compared in terms of adhesive strength, specific interaction, and chain orientation at the interface. It has been found that at low comonomer contents the SAA shows higher adhesive strength than S4VP, but the situation becomes reversed at higher comonomer contents. Now a question may arise as to which functionality is more effective for the adhesion with metal when both two functionalities are present in the same polymer chain.

In this study, we investigate the competitive adsorption behavior of the two functionalities in the same chain onto metal surfaces using adhesive strength measurement, reflection–absorption infrared spectroscopy, and XPS. Here, poly(methyl methacrylate-*co*-4-vinylpyridine) (MMA4VP) and poly(methyl methacrylate-*co*-2-vinylpyridine) (MMA2VP) random copolymers are used as model copolymers that contain both nitrogen- and oxygen-containing functionality in the same chain, and their adsorption behaviors onto alumina are examined as a function of copolymer composition.

Experimental Section

Synthesis of Copolymers. Poly(methyl methacrylate-*co*-4-vinylpyridine) (MMA4VP) and poly(methyl methacrylate-*co*-2-vinylpyridine) (MMA2VP) random copolymers containing

* To whom correspondence should be addressed. Tel +82-2-880-7192; Fax +82-2-885-1748; e-mail whjpoly@plaza.snu.ac.kr.

Table 1. Properties of Copolymers

designation	VP content (mol %)	T_g (°C)	$[\eta]$ (dL/g)
MMA2VP8	77.1	100	0.29
MMA2VP5	52.5	102	0.36
MMA2VP2	18.2	104	0.44
MMA4VP8	81.9	121	0.17
MMA4VP5	48.3	124	0.20
MMA4VP2	23.5	129	0.34

20–80 mol % VP were synthesized in a sealed glass ampule by bulk free radical copolymerization at 60 °C, using 2,2-azobis(isobutyronitrile) (AIBN) as an initiator. The monomer reactivity ratios (r_i) are reported as follows:¹⁸ $r_{\text{MMA}} = 0.57$, $r_{4\text{VP}} = 0.77$; $r_{\text{MMA}} = 0.35$, $r_{2\text{VP}} = 0.76$. The copolymer composition was determined by the titration method,^{19,20} and the properties of the copolymers are listed in Table 1.

Preparation of Metal Substrate. The aluminum metal used in this study is a commercial product (DaeHan Aluminum Co., Al1050) of 99.9% purity. Metal substrates for reflection–absorption infrared (RAIR) spectroscopy and X-ray photoelectron spectroscopy (XPS) were prepared as follows.²¹ Aluminum plates with a thickness of 1.5 mm were mechanically polished with a series of dry silicon carbide abrasive papers ranging from 320 to 2000 grit. After the surface was grounded, wet polishing was performed using 0.05 μm alumina powder in Microcloths (Buehler Inc.) with deionized water as a lubricant. The resulting mirrors were ultrasonically rinsed with deionized water and dried by blowing with nitrogen gas. As substrates for adhesion, sheets of aluminum of size $100 \times 25 \times 1 \text{ mm}^3$ were mechanically polished as described above. The grounded metal sheets were etched by 20% hydrochloric acid solution for 1 min to remove the oxide layer on the surface. The resulting plates were ultrasonically washed with acetone, followed by rinsing the plates with deionized water, and then dried by blowing with nitrogen gas.

Adhesion Strength Measurement. Test specimens were prepared by applying a film of 5% polymer solution to the end of one metal plate, and another plate was placed onto the film so that lap area would be $25 \times 15 \text{ mm}^2$. The assembly was tightly clamped and cured at 110 °C for 1 h. The adhesive strength was measured by the lap shear test (ASTM D1092-72) at a pull rate of 5 mm/min, using a universal tensile machine (LLOYD, LR 10K). The lap shear strength was calculated by dividing the strength by the lap area. Five sets of specimens for each polymer were tested, and the average data are reported as the lap shear strength.

Infrared Spectroscopy. The bulk spectra of polymers were recorded on a Fourier transform infrared spectrometer (FTIR, Perkin-Elmer 1760X) at a resolution of 4 cm^{-1} , and 32 scans were collected. Samples for reflection–absorption infrared (RAIR) spectroscopy were prepared by immersing the prepared aluminum substrate into 2% polymer solution in chloroform for 1 h, and after removal of the sample from the solution, the solvent was slowly evaporated. The RAIR spectra of polymer/metal interface were obtained using a Bomem MB-100 spectrometer at a resolution of 4 cm^{-1} with 100 scans. A Graseby Spec P/N 19650 monolayer/grazing angle accessory was used. The angle of incidence was 78°, and freshly polished copper and aluminum substrates were used for the reference spectrum.

X-ray Photoelectron Spectroscopy. Preparation of sample for X-ray photoelectron spectroscopy (XPS) was identical to that for RAIR spectroscopy. The XPS measurements were performed on a Surface Science Instruments spectrometer (SSI, 2803-S) equipped with a monochromatic Al K α X-ray source at a power of 200 W. The pass energy was 44.75 eV (0.5 eV steps) and 17.90 eV (0.05 eV steps) for the survey and high-resolution spectra, respectively. The pressure in the chamber was approximately 1×10^{-9} Torr. A takeoff angle of 90° relative to the surface plane was used to obtain all spectra. All the XPS spectra were corrected for charging effect by referencing the C 1s peak of hydrocarbons to 285.0 eV. High-resolution spectra were analyzed in order to determine the various chemical species present. Each spectrum was curve

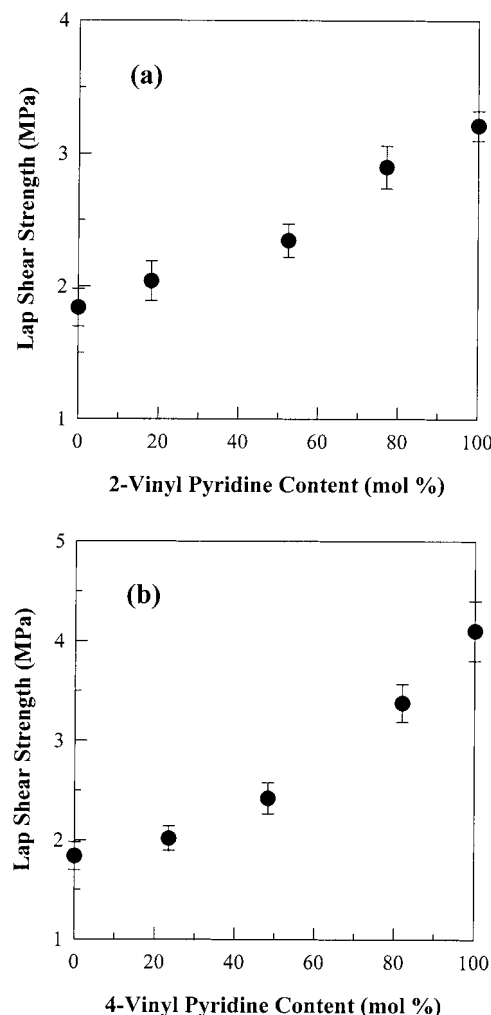


Figure 1. Lap shear strength between copolymers and alumina as a function of copolymer composition: (a) MMA2VP/alumina; (b) MMA4VP/alumina.

fitted using the XPSPEAK2 software. Quantification of XPS spectra was achieved by curve integration using a nonlinear baseline and by correcting the integrated area using elemental sensitivity factors. For quantitative analysis, spectra for all the samples were recorded for the same scan time. To examine the polymer/metal interface, the polymer overlayer was sputtered until characteristic peaks of aluminum appear, and then the spectra were recorded.

Film Thickness Measurements. Film thickness upon metal substrates used for the RAIR spectroscopy and XPS was determined by ellipsometry (Rudolph Auto EL-II). The refractive index of the copolymer was assumed to be 1.50.

Results and Discussion

The adhesive strength between poly(methyl methacrylate-*co*-2-vinylpyridine) (MMA2VP)/alumina and between poly(methyl methacrylate-*co*-4-vinylpyridine) (MMA4VP)/alumina is measured as a function of copolymer composition, as shown in Figure 1. The adhesive strength increases with increasing the 2VP or 4VP comonomer content in both copolymers. This suggests that the nitrogen-containing functionality plays a more important role in enhancing the adhesive strength between the model copolymers and alumina. When the adhesive strength of MMA2VP/alumina system is compared with that of MMA4VP/alumina system, it can be seen that the adhesive strength of MMA4VP/alumina system is slightly greater than that of MMA2VP/

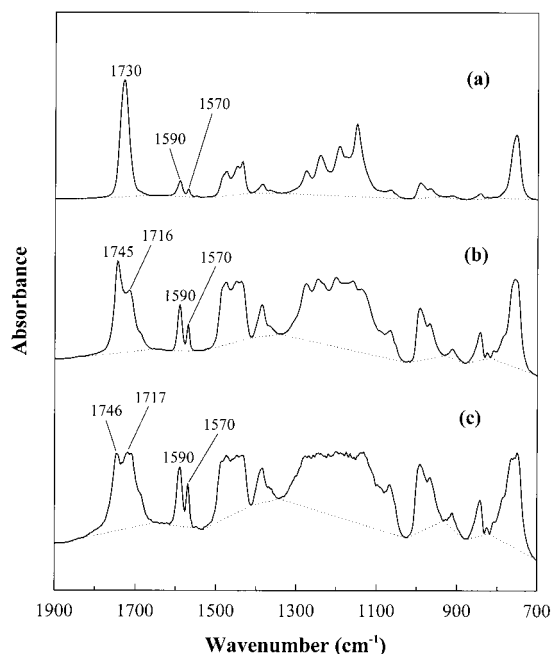


Figure 2. (a) Transmission IR spectrum of MMA2VP2. (b) RAIR spectrum of MMA2VP2 adsorbed on alumina from 2% solution in chloroform. (c) RAIR spectrum of MMA2VP2 adsorbed on alumina from 0.75% solution in chloroform.

alumina system, indicating that the 4VP unit is more effective than 2VP unit in enhancing the adhesion to alumina substrate. Here it is important to investigate where the failure of the joints occurs. To confirm the locus of failure, we examined the surface of metal side after fracture by XPS and RAIR. Several points of the metal side after measurement of the lap shear strength were examined by XPS. Characteristic peaks of aluminum (Al 2s, Al 2p) were observed with very small peaks from the copolymer (C 1s, O 1s) in the spectrum of metal side after fracture. Such a failure profile suggests that the failure did not occur within the inner layer of copolymer. The surface of metal side after fracture was examined also by RAIR spectroscopy. We were not able to obtain any complete spectrum characteristic of the copolymer, indicating that the fracture of the adhesive joint occurs mainly at the interface between the copolymer and metal.

To investigate the nature of adhesion between the copolymers and alumina substrate, the transmission IR spectroscopy and RAIR spectroscopy were used for bulk spectrum and interface spectrum, respectively. Figure 2 shows the transmission IR spectrum of poly(methyl methacrylate-*co*-2-vinylpyridine) (MMA2VP2) and the RAIR spectrum of MMA2VP2 adsorbed onto alumina substrate from 2% solution in chloroform. In Figure 2a, the MMA2VP2 copolymer has characteristic absorption bands at 1730, 1590, and 1570 cm^{-1} . The band at 1730 cm^{-1} corresponds to C=O stretching of the MMA unit, and the bands at 1590 and 1570 cm^{-1} are attributed to coupled C=C and C=N stretching mode of the pyridine ring.²⁰ When the MMA2VP2 is adsorbed onto alumina, the band at 1730 cm^{-1} splits into two peaks at 1745 and 1716 cm^{-1} , as shown in Figure 2b. The appearance of a lower shifted peak at 1716 cm^{-1} indicates that free carbonyl groups in MMA units interact specifically with alumina. The unusual shift to a higher frequency of 1745 cm^{-1} can be explained in two ways. If a significant degree of dipole-dipole interactions exists among MMA carbonyl groups, there exist two distinct populations of

carbonyl groups, i.e., the free and self-associating ones. The interaction between carbonyl groups in MMA units and alumina may cause the disruption of self-association between carbonyl groups, resulting in the carbonyl band shift to a higher frequency region.²² Another possibility for the upper shift may arise from a significant contribution of the refractive index to the reflectivity of a sample coupled with the rapid changes in the refractive index in the region of an absorption band.^{23,24} The two mechanisms described above may explain the upper shift of the 1731 cm^{-1} band to 1745 cm^{-1} , as shown in Figure 2. Unlike the carbonyl stretching band, the C=C and C=N stretching bands at 1590 and 1570 cm^{-1} do not shift in the RAIR spectra obtained from MMA2VP2 adsorbed on alumina, as shown in Figure 2b. However, it is noteworthy that the relative intensities of the C=C and C=N bands become stronger in the RAIR spectra as compared with the intensity of the carbonyl band at 1745 cm^{-1} . Since the RAIR spectroscopy is very sensitive to preferential orientation of functional groups at the surface of a metal, i.e., vibrational modes with transition moments perpendicular to the surface of the substrate appear with much stronger intensity than do vibrations with transition moments parallel to the surface, the difference between the transmission and the RAIR spectrum may come from the orientation difference of functional groups.²⁵⁻²⁷ From the selective increase in intensity of the coupled C=C and C=N stretching of pyridine ring in RAIR spectra, it is inferred that the pyridine rings in VP units adsorbed onto metal surface are more oriented in a vertical direction than the carbonyl groups in MMA units. This may explain why the adhesive strength of the MMA2VP/alumina and MMA4VP/alumina systems increases with increasing VP composition in copolymers.

Parts a and b of Figure 3 show the transmission IR spectrum of poly(methyl methacrylate-*co*-4-vinylpyridine) (MMA4VP2) and the RAIR spectrum obtained from MMA4VP2 adsorbed onto alumina substrate from 2% solution in chloroform, respectively. Like the case of MMA2VP2/alumina, when the MMA4VP2 is adsorbed onto alumina, the C=O stretching band of MMA unit at 1730 cm^{-1} also splits into two bands at 1745 and 1710 cm^{-1} , as shown in Figure 2. It is also observed that the intensity of the bands at 1600 and 1558 cm^{-1} (Figure 3b), which correspond to coupled C=C and C=N stretching mode in pyridine ring, respectively, becomes relatively stronger as compared with the intensity of the carbonyl band at 1745 cm^{-1} .

A question may arise that the film thickness for Figures 2b and 3b is thick to obtain information on the interface, making the interpretation of the carbonyl band splitting questionable. To eliminate such an effect, thinner films were prepared from 0.75% solution onto alumina, and their RAIR spectra (Figures 2c and 3c) are examined. It is known that the interface region makes an increasing contribution to the overall spectrum as the film becomes thinner.^{38,39} As the film thickness becomes thinner, the splitting of carbonyl band becomes more apparent as can be seen in Figures 2 and 3. It is also observed that the intensities of the coupled C=C and C=N bands become stronger in thinner films (Figures 2c and 3c) than in thicker films (Figures 2b and 3b).

The adsorption behavior of the copolymers with higher content of VP is investigated. When MMA2VP5 and MMA4VP5 are adsorbed on alumina surfaces, it is

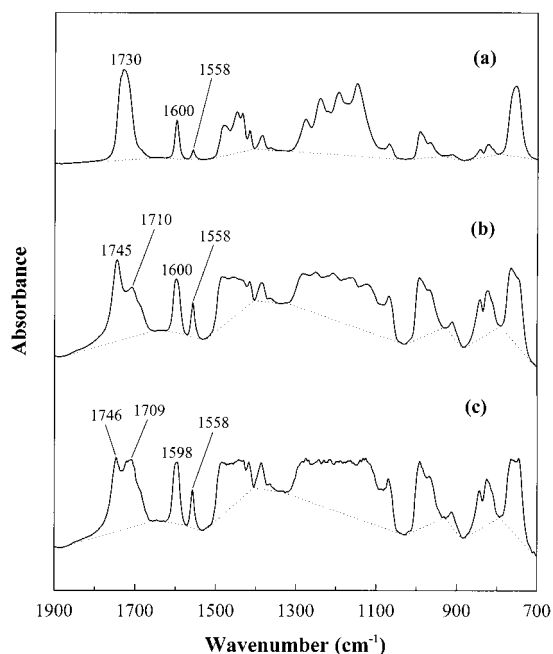


Figure 3. (a) Transmission IR spectrum of MMA4VP2. (b) RAIR spectrum of MMA4VP2 adsorbed on alumina from 2% solution in chloroform. (c) RAIR spectrum of MMA4VP2 adsorbed on alumina from 0.75% solution in chloroform.

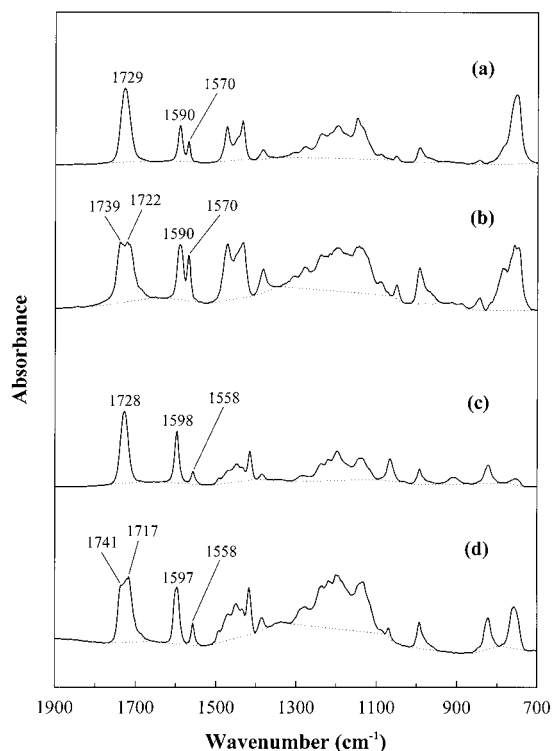


Figure 4. (a) Transmission IR spectrum of MMA2VP5. (b) RAIR spectrum of MMA2VP5 adsorbed on alumina from 0.75% solution in chloroform. (c) Transmission IR spectrum of MMA4VP5. (d) RAIR spectrum of MMA4VP5 adsorbed on alumina from 0.75% solution in chloroform.

also observed that the C=O stretching band splits into two peaks and that the intensities of the coupled C=C and C=N stretching mode become stronger as compared with that of carbonyl band, as shown in Figure 4.

For quantitative comparison of RAIR spectra of samples with different film thickness and VP content, the quantitative absorption–reflection thickness IR

Table 2. Changes of Equivalent Thickness-Normalized Band Absorbances with Different Film Thickness and VP Content

	film thickness (nm) ^a	thickness-normalized band absorbance ^b	
		C=O stretching band	C=C and C=N stretching band
MMA2VP2	bulk	0.160	0.019
2%	11.7	0.171	0.029
0.75%	6.8	0.213	0.038
MMA4VP2	bulk	0.173	0.031
2%	16.2	0.187	0.052
0.75%	4.8	0.245	0.087
MMA2VP5	bulk	0.145	0.058
0.75%	5.2	0.181	0.076
MMA4VP5	bulk	0.149	0.066
0.75%	8.4	0.211	0.098

^a Measured by ellipsometry. ^b Particular band absorbance divided by spectral-average band absorbance.

(QUARTIR) method is used.³⁸ A possible alternative measure of film thickness is to use the spectral average absorbance, since RAIR band intensities are expected to vary monotonically if not linearly with film thickness. Absorbances of carbonyl bands (or coupled C=C and C=N stretching bands) are normalized with respect to the constant equivalent thickness, obtained from the average absorbance of major bands. Changes in relative band intensity observed in going from thick to thinner films represent the orientation of the functional groups at the interface. Table 2 summarizes the results obtained from Figures 2–4, where the baselines used in determining the absorbances are indicated as dotted lines in the spectra. The normalized absorbance of both the C=O stretching band and the coupled C=C and C=N stretching band increases with decreasing film thickness, as shown in Table 2, indicating that the carbonyl group and pyridine ring are oriented more vertically to the metal substrate. It is also noteworthy that the increase of the normalized absorbance of C=C and C=N bands is slightly larger (34% increase from 0.029 to 0.038) than that of C=O band (25% increase from 0.171 to 0.213) for MMA2VP2 as the film thickness decreases. This trend is more apparent for MMA4VP2, i.e., 49% increase of C=C and C=N stretching band (from 0.052 to 0.087) versus 31% increase of C=O stretching band (from 0.187 to 0.245). This leads us to conclude that 4VP unit is oriented more vertically to the interface than 2VP unit. This behavior is also observed for MMA2VP5 and MMA4VP5, as shown in Table 2.

The XPS investigation is used to quantitatively analyze the competitive adsorption behavior between MMA units and 2VP (or 4VP) units upon alumina substrate. The XPS survey spectra of MMA2VP5 bulk and the MMA2VP5/alumina interface are shown in Figure 5. Three peaks corresponding to C 1s, O 1s, and N 1s electrons are observed in the MMA2VP5 bulk spectrum (Figure 5a), and two additional lines which are characteristic peaks of aluminum are observed in the MMA2VP5/alumina interface spectrum (Figure 5b). A simple inspection of Figure 5 shows that the intensities of O 1s and N 1s peaks at the interface are relatively larger compared to those of the polymer bulk, which implies that the oxygen and nitrogen atoms are predominantly located at the interfacial region.

Parts a and b of Figure 6 show the high-resolution C 1s spectra obtained from the MMA2VP5 bulk and the MMA2VP5/alumina interface, respectively. The spectrum of the MMA2VP5 bulk consists of four types of

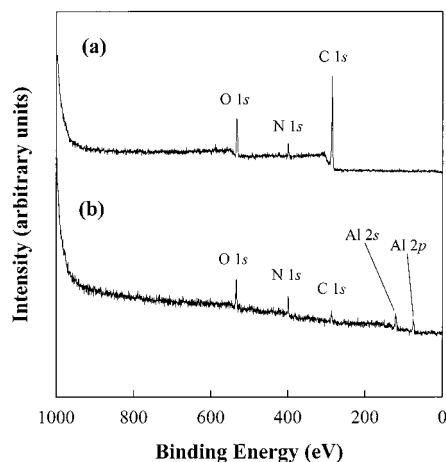


Figure 5. XPS survey spectra of MMA2VP5 bulk (a) and MMA2VP5/alumina interface (b).

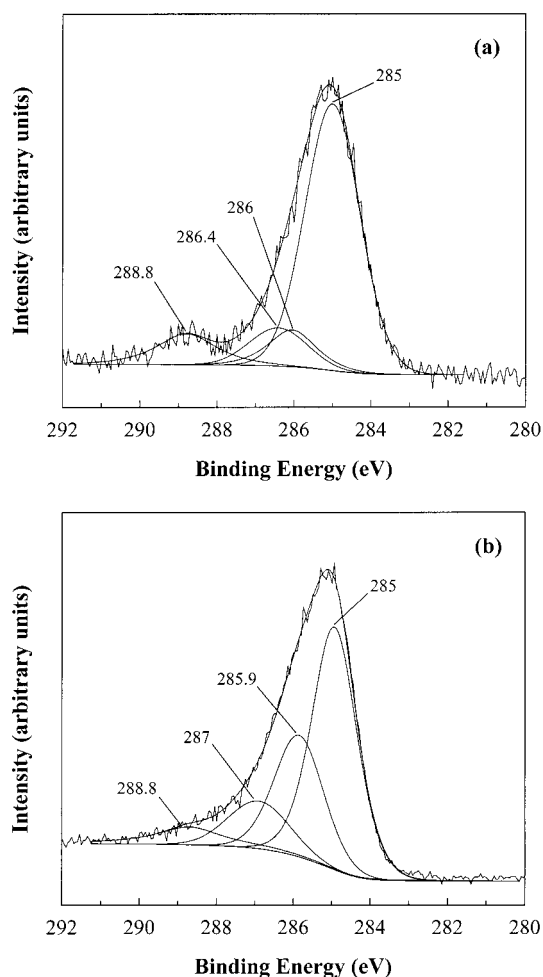


Figure 6. XPS high-resolution C 1s spectra of MMA2VP5 bulk (a) and MMA2VP5/alumina interface (b).

carbon atoms which can be assigned as C–C or C–H carbon at 285 eV, C–N (or C=N) carbon at 286 eV, C–O carbon at 286.4 eV, and C=O carbon at 288.8 eV.^{40,41}

The C 1s spectrum from the MMA2VP5/alumina interface is decomposed into four peaks at 285, 285.9, 287, and 288.8 eV. When this interface spectrum (Figure 6b) is compared with the bulk spectrum (Figure 6a), it is realized that a large amount of the carbonyl C 1s peak at 288.8 eV in the bulk spectrum shifts to lower binding energy at 287 eV and a small amount of C 1s peak still

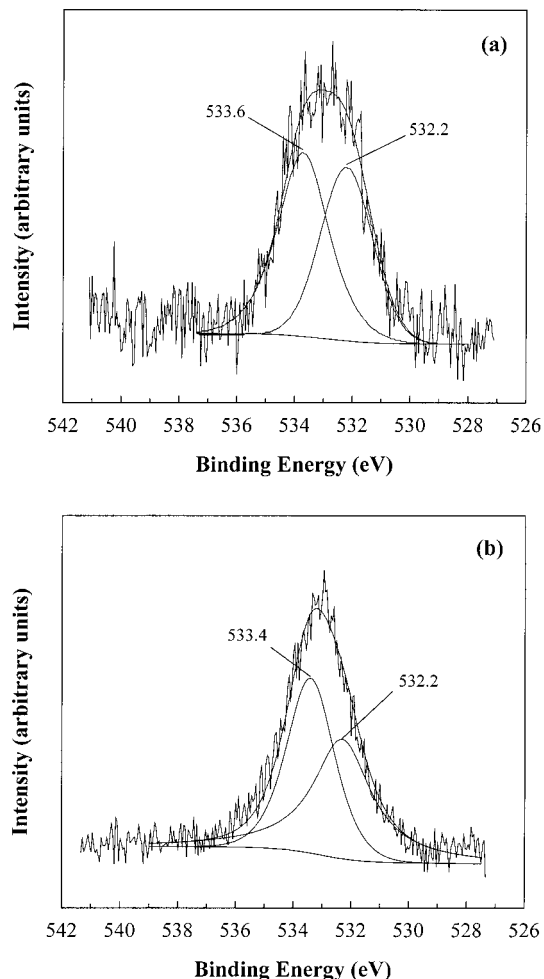


Figure 7. XPS high-resolution O 1s spectra of MMA2VP5 bulk (a) and MMA2VP5/alumina interface (b).

remains at 288.8 eV in the interface spectrum. This indicates that there is a specific interaction between the carbonyl group in the MMA unit and alumina. Here the difference of chemical shift between C–N (or C=N) carbon at 286 eV and C–O carbon at 286.4 eV of the bulk spectrum is too small to be identified in the interface spectrum by curve fitting. These two peaks of the bulk spectrum are merged into a single peak centered at 285.9 eV with enhanced peak intensity, as shown in Figure 6b.

The specific interaction between MMA2VP5 and alumina is also supported by the analysis of O 1s spectra. As shown in Figure 7a, the O 1s spectrum of the MMA2VP5 bulk is decomposed into two components at 532.2 and 533.6 eV which can be assigned to be C=O and C–O oxygen, respectively. Since both types of oxygen atom are of equal amount, the area of the two O 1s peaks should almost be equal (Figure 7a). When the MMA2VP5 is adsorbed onto alumina, some noticeable changes in O 1s spectra can be observed as follows. The shape of carbonyl O 1s peak becomes broader in the interface spectrum, and the ratio of the C=O peak intensity to C–O peak intensity increases from 0.93 at the polymer bulk spectrum (Figure 7a) to 1.1 at the polymer/metal interface spectrum (Figure 7b). This result suggests that the amount of carbonyl oxygen atom increases near the interface due to the specific interaction between carbonyl oxygen in the MMA unit and aluminum. The absence of an expected shift in the O

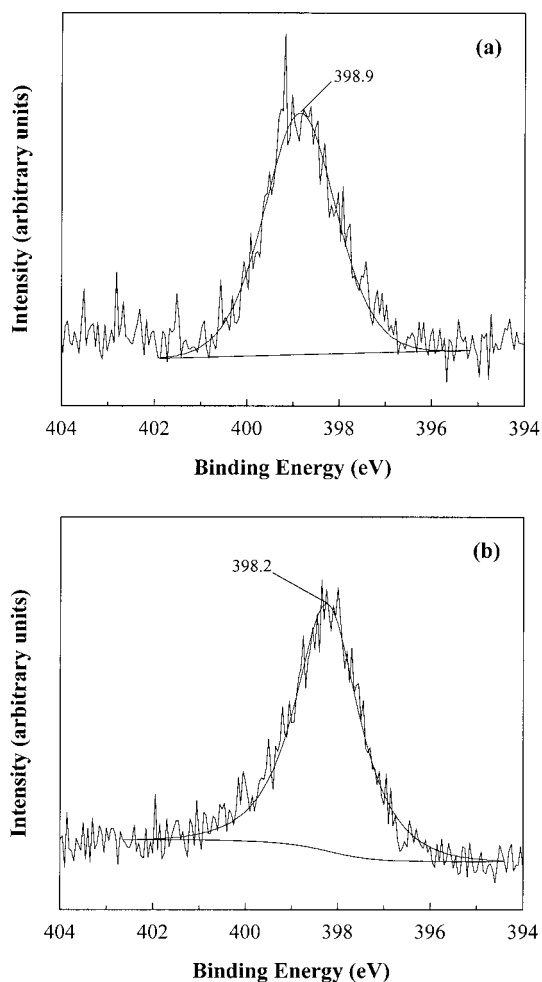


Figure 8. XPS high-resolution N 1s spectra of MMA2VP5 bulk (a) and MMA2VP5/alumina interface (b).

1s peak in Figure 7b can be explained by a charge delocalization from oxygen to carbon concurrent with interaction.^{42,43}

Examination of the N 1s spectra can provide further insights into the interaction between MMA2VP5 and alumina. The N 1s spectrum from the bulk consists of only one component, centered at 398.9 eV, as shown in Figure 8a. When the N 1s spectrum from the bulk is compared with that from the interface, the N 1s peak at 398.9 eV shifts to lower binding energy (398.2 eV) at the interface spectrum (Figure 8b). This suggests that the 2VP units in the MMA2VP5 can also interact specifically with alumina. At the interface between the MMA2VP5 and the alumina, the electron density in the nitrogen atom in the pyridine ring increases due to the transfer of electrons from alumina to 2VP unit because of interaction, and therefore the electron binding energy in the nitrogen atom shifts to a low binding energy level, as reported in the literature.^{44–48} It is comparable that the N 1s spectrum shifts to 0.5 and 1.0 eV lower binding energy upon adsorption of polyimide onto gold and copper substrates.⁴⁹

The interaction between MMA4VP5 and alumina is also examined by XPS. Similar to the case of MMA2VP5, C 1s, O 1s, and N 1s lines are observed in the survey spectrum of MMA4VP5 bulk while two additional lines characteristic of alumina appear in the MMA4VP5/alumina interface spectrum, as shown in Figure 9. It is clear that the relative intensities of O 1s and N 1s peaks

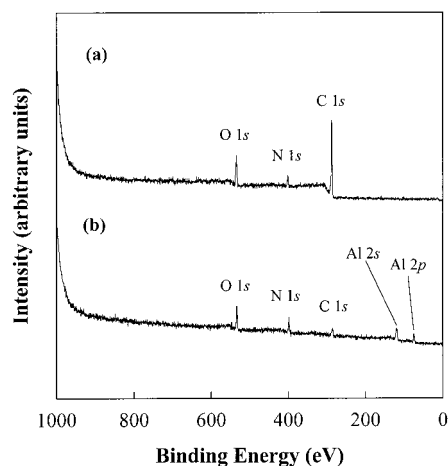


Figure 9. XPS survey spectra of MMA4VP5 bulk (a) and MMA4VP5/alumina interface (b).

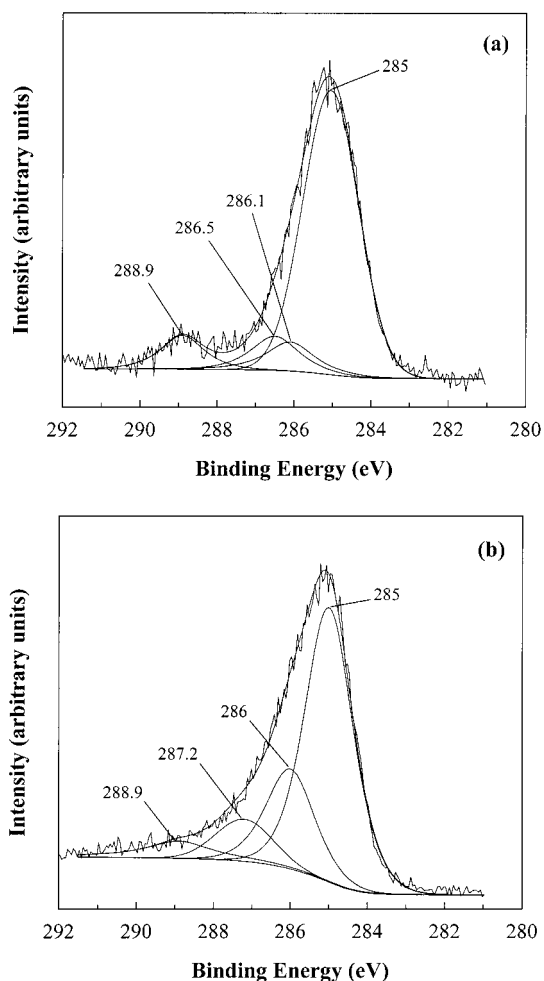


Figure 10. XPS high-resolution C 1s spectra of MMA4VP5 bulk (a) and MMA4VP5/alumina interface (b).

in the interface spectrum are also larger compared to those of the bulk spectrum, indicating that the oxygen and nitrogen atoms in the copolymer interact specifically with alumina. Similar to the high-resolution spectrum of MMA2VP5 bulk (Figure 6a), the C 1s spectrum of MMA4VP5 bulk consists of four characteristic peaks (Figure 10a). The specific interaction between carbonyl group in MMA4VP5 and alumina can also be confirmed by the shift of the carbonyl C 1s peak at 288.9 eV to lower binding energy, hence resulting in a new broad

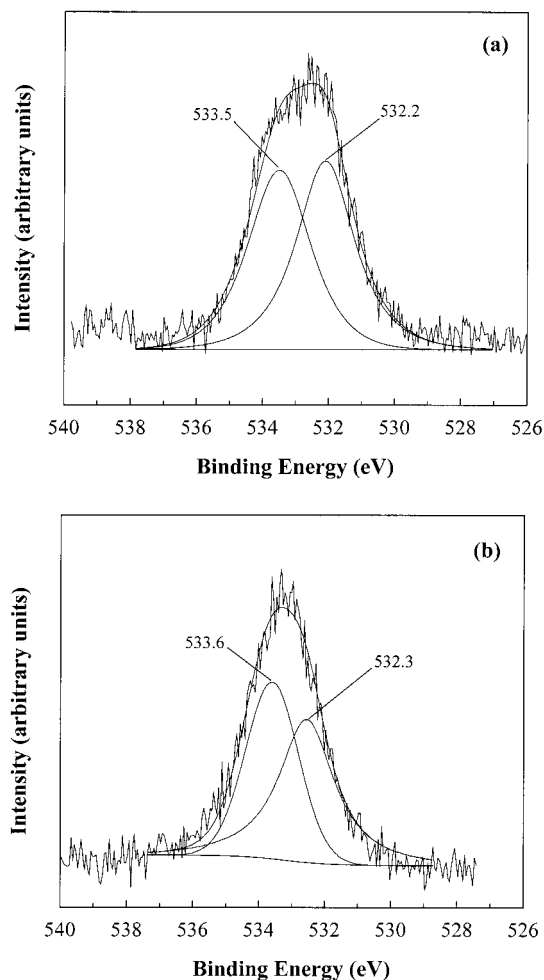


Figure 11. XPS high-resolution O 1s spectra of MMA4VP5 bulk (a) and MMA4VP5/alumina interface (b).

peak at 287.2 eV (Figure 10b) in the interface spectrum. Comparison of the O 1s spectrum of MMA4VP5 bulk with that of MMA4VP5/alumina interface spectrum also supports the interaction between carbonyl oxygen in MMA4VP5 and alumina, i.e., the ratio of C=O peak intensity to C–O peak intensity increases from 1.0 in the bulk spectrum (Figure 11a) to 1.1 in the interface spectrum (Figure 11b). Like the case with MMA2VP2, comparison of the N 1s spectrum of the MMA4VP5 bulk (Figure 12a) with that of the MMA4VP5/alumina interface (Figure 12b) indicates that the N 1s peak at 399 eV shifts to a lower binding energy (398.1 eV) at the interface spectrum, indicating that the 4VP unit can also interact with alumina. These results lead us to conclude that the MMA4VP5 also interacts with alumina surface through both the carbonyl oxygen atoms in MMA units and the nitrogen atoms in the 4VP units.

To examine competitive adsorption behavior between oxygen- and nitrogen-containing functionality in the

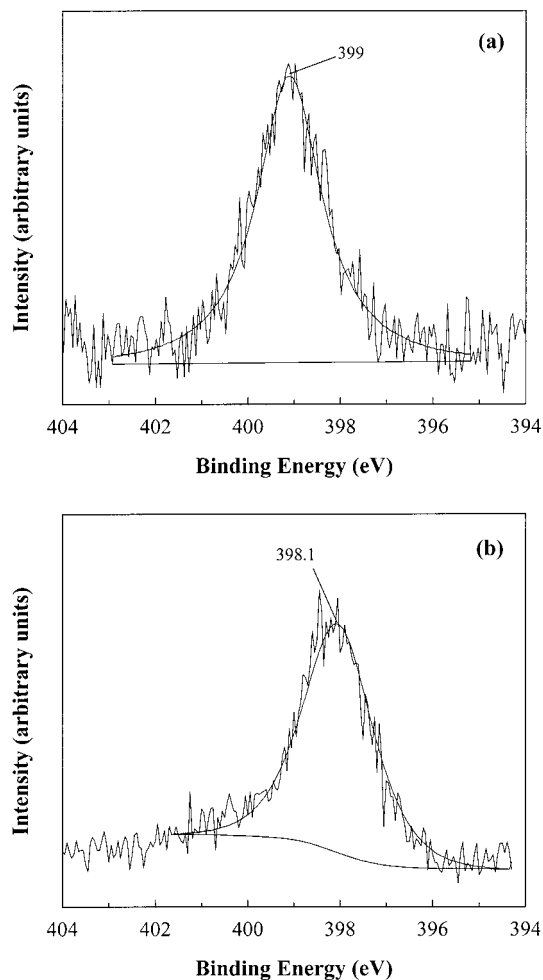


Figure 12. XPS high-resolution N 1s spectra of MMA4VP5 bulk (a) and MMA4VP5/alumina interface (b).

same chain onto alumina surface, we have quantitatively analyzed the XPS data. Table 3 lists normalized C 1s, O 1s, and N 1s peak areas and relative percent amounts of each component calculated from the high-resolution spectra of the copolymer bulk and the copolymer/alumina interface. The atomic percentage of each element obtained by the bulk spectrum agrees well with the value calculated theoretically from the chemical structure of repeating unit. The relative amounts of oxygen and nitrogen atoms at the polymer/metal interface are significantly higher than those at the bulk, indicating that there are specific interactions between both functional groups and alumina. To directly examine competitive adsorption behavior between oxygen- and nitrogen-containing functional groups, the relative percent areas of O 1s and N 1s peaks in the interface spectrum are divided by their respective percent areas of the bulk spectrum, and the values are listed in Table 2. For the MMA2VP5, the relative amount of nitrogen adsorbed onto alumina is 3.9 times the amount of

Table 3. Normalized Areas and Atomic Compositions Obtained by the XPS High-Resolution Spectra for the Polymer Bulk and Polymer/Metal Interface

	MMA2VP55/aluminum			MMA4VP55/aluminum		
	C 1s	O 1s	N 1s	C 1s	O 1s	N 1s
polymer bulk	1211	253	157	1290	252	157
	74.7%	15.6%	9.7%	75.9%	14.9%	9.2%
polymer/metal interface	298	431	443	334	447	522
	25.4%	36.8%	37.8%	25.4%	34.3%	40.3%
interface/bulk	0.3	2.4	3.9	0.3	2.3	4.4

polymer bulk (from 9.7% to 37.8%), whereas the amount of oxygen adsorbed onto alumina is 2.4 times the amount of polymer bulk (from 15.6% to 36.8%). Similar results are observed for the MMA4VP5/alumina system. These results indicate that the nitrogen-containing functionality is adsorbed more selectively onto alumina surface than the oxygen-containing functionality for both the MMA2VP5/alumina and MMA4VP5/alumina systems. This is consistent with the results of adhesive strength measurement. It should be mentioned here that an oxide layer may be formed upon the aluminum substrate although the substrate was polished as we described in the Experimental Section. Consequently, the percent area of O 1s peak at the interface may come in part from the aluminum oxide. Therefore, the relative percentage areas of the O 1s from the copolymers must be smaller than the values in Table 3. This fact reinforces the conclusion that the nitrogen-containing functionality is more selectively adsorbed onto alumina surface than the oxygen-containing functionality. Another feature of note from Table 3 is that the 4VP unit is adsorbed slightly more favorably onto alumina substrate than the 2VP unit, which may explain that the adhesive strength of the MMA4VP5/alumina system is larger than that of MMA2VP5/alumina system.

Conclusions

Competitive adsorption behavior between oxygen- and nitrogen-containing functionality in model copolymer onto alumina substrate was investigated using RAIR spectroscopy and XPS. The adhesive strength of both the MMA2VP/alumina and MMA4VP/alumina systems increased with increasing 2VP (or 4VP) content in copolymers, and this effect was more prominent for the MMA4VP/alumina system. RAIR spectroscopy indicates that the oxygen-containing functionality in MMA2VP (or MMA4VP) interacts specifically with alumina, which is clearly identified by the shift of the carbonyl band to lower frequency regions. The selective increase in intensity of the characteristic bands of pyridine ring in the RAIR spectrum, as compared with that of carbonyl band, indicates that the pyridine rings in copolymers are more oriented in a perpendicular direction to the metal surface than carbonyl groups in the same chain. This observation is confirmed by QUARTIR analysis.

The specific interaction between aluminum and oxygen-containing functionality in MMA units or nitrogen-containing functionality in vinylpyridine units was confirmed by XPS. The carbonyl C 1s peak and the N 1s peak of the polymer bulk spectra shift to lower binding energies in the polymer/metal interface spectra for both the MMA2VP5/alumina and MMA4VP5/alumina systems. The lower shifts of carbonyl C 1s peak and pyridine N 1s peak indicate that electrons in aluminum transfer to the adsorbed molecules as a result of specific interaction.

Quantitative analysis of XPS spectra reveals that the ratio of N 1s peak areas of the interface spectrum to those of the bulk spectrum is higher than the ratio of O 1s peak areas to those of the bulk spectrum for both MMA4VP/alumina and MMA2VP/alumina systems. This indicates that the nitrogen-containing functionality adsorbs more favorably onto alumina surface than the oxygen-containing functionality. This result is consistent with the results of the adhesive strength measurement and RAIR spectroscopy.

Finally, it should be noted that our conclusions could apply only to the model copolymers (MMA2VP or MMA4VP)/alumina systems in which the oxygen- and nitrogen-containing functionality are not sterically identical to have access to the metal substrate. Therefore, further experiments are necessary to provide a general picture as to which functionality would play a predominant role in competitive adsorption behavior of the two functionalities in the same chain onto metal surfaces.

Acknowledgment. The authors thank the Ministry of Education, the Republic of Korea, for their financial support through the Research Fund for Advanced Materials in 1997.

References and Notes

- (1) Sabatini, E.; Boulakia, J. C.; Bruening, M.; Rubinstein, I. *Langmuir* **1989**, *9*, 2974.
- (2) Ulman, A. *An Introduction to Ultrathin Organic Films from Langmuir–Blodgett to Self-Assembly*; Academic Press: New York, 1991.
- (3) Napper, D. H. *Polymeric Stabilization of Colloidal Dispersions*; Academic Press: London, 1983.
- (4) Xue, G.; Dong, J.; Zhang, J. *Macromolecules* **1991**, *24*, 4195.
- (5) Lee, K. W.; Walker, G. W.; Viehbeck, A. In *Fundamentals of Adhesion and Interface*; Rimai, D. S., DeMejo, L. P., Mittal, K. L., Eds.; VSP: Utrecht, 1995; pp 161–177.
- (6) Xue, G.; Dong, J.; Wu, P. *J. Polym. Sci., Polym. Phys.* **1992**, *30*, 1097.
- (7) Roth, P. G.; Boerio, F. J. *J. Polym. Sci., Polym. Phys.* **1987**, *25*, 1923.
- (8) Lu, Y.; Xue, G. *Polymer* **1993**, *34*, 3750.
- (9) Xue, G.; Dong, J. *Polymer* **1992**, *33*, 643.
- (10) Ansarifard, M. A.; Luckham, P. F. *Polymer* **1988**, *29*, 329.
- (11) Venkatachalam, R. S.; Boerio, F. J.; Roth, P. G.; Tsai, W. H. *J. Polym. Sci., Polym. Phys.* **1988**, *26*, 2447.
- (12) Lippert, J. L.; Brandt, E. S. *Langmuir* **1988**, *4*, 127.
- (13) Garrel, R. L.; Beer, K. D. *Langmuir* **1989**, *5*, 452.
- (14) Burkstrand, J. M. *J. Vac. Sci. Technol.* **1982**, *20*, 440.
- (15) Burkstrand, J. M. *J. Appl. Phys.* **1981**, *52*, 4795.
- (16) Burkstrand, J. M. *J. Vac. Sci. Technol.* **1979**, *16*, 363.
- (17) Kim, D. H.; Jo, W. H. *Polymer* **1999**, *40*, 3889.
- (18) Brandrup, J.; Immergut, E. H. *Polymer Handbook*, 3rd ed.; John Wiley and Sons: New York, 1989; p 199.
- (19) Tamikado, T. *J. Polym. Sci.* **1960**, *18*, 489.
- (20) Jo, W. H.; Lee, S. C.; Lee, M. S. *Polym. Bull.* **1989**, *21*, 183.
- (21) Young, J. T.; Boerio, F. J. *Surf. Interface Anal.* **1993**, *20*, 341.
- (22) Jo, W. H.; Cruz, C. A.; Paul, D. R. *J. Polym. Sci., Polym. Phys.* **1989**, *27*, 1057.
- (23) Allara, D. L.; Baca, A.; Pryde, C. A. *Macromolecules* **1978**, *11*, 1215.
- (24) Harric, N. J. In *Characterization of Metal and Polymer Surfaces*; Lee, L. H., Ed.; Academic Press: New York, 1977; Vol. 2, pp 153–192.
- (25) Greenler, R. G. *J. Chem. Phys.* **1966**, *44*, 310.
- (26) Moskovits, M. *J. Chem. Phys.* **1982**, *77*, 4408.
- (27) Boerio, F. J.; Chen, S. L. *Appl. Spectrosc.* **1979**, *33*, 121.
- (28) Tsai, W. H.; Boerio, F. J.; Jackson, K. M. *Langmuir* **1992**, *8*, 1443.
- (29) Sun, F.; Grainger, D. W.; Castner, D. G.; Leach-Scampavia, D. K. *Macromolecules* **1994**, *27*, 3053.
- (30) Sun, F.; Grainger, D. W. *J. Polym. Sci., Polym. Chem.* **1993**, *31*, 1729.
- (31) Hoffman, C. L.; Rabolt, J. F. *Macromolecules* **1996**, *29*, 2543.
- (32) Tsao, M. W.; Dfeifer, K. H.; Rabolt, J. F.; Castner, D. G.; Haussliag, L.; Ringsdorf, H. *Macromolecules* **1997**, *30*, 5913.
- (33) Lenk, T. J.; Hallmark, V. M.; Rabolt, J. F.; Haussliag, L.; Ringsdorf, H. *Macromolecules* **1993**, *26*, 1230.
- (34) Biebuyik, H. A.; Whitesides, G. M. *Langmuir* **1993**, *9*, 1230.
- (35) Steiner, U. B.; Rehahn, M.; Caseri, W. R.; Suter, U. W. *Langmuir* **1995**, *11*, 3013.
- (36) Steiner, U. B.; Caster, W. R.; Suter, U. W. *Langmuir* **1993**, *9*, 3245.
- (37) Linde, H. G. *J. Appl. Polym. Sci.* **1992**, *46*, 353.
- (38) Debe, M. K. *Appl. Surf. Sci.* **1982**, *14*, 1.
- (39) Debe, M. K. *J. Vac. Sci. Technol.* **1982**, *21*, 74.
- (40) Briggs, D.; Seah, M. P. *Practical Surface Analysis*; John Wiley and Sons: Chichester, 1983; Vol. 1.

- (41) Chan, C. M. *Polymer Surface Modification and Characterization*; Hanser Publisher: New York, 1994.
- (42) Domingue, A.; Bailey, L. D.; Sacher, E.; Yelon, A.; Ellis, T. H. In *Metallization of Polymers*; Sacher, E., Pireaux, J. J., Kowalczyk, S. P., Eds.; ACS Symposium Series 440; American Chemical Society: Washington, DC, 1990; pp 272–287.
- (43) Bou, M.; Martin, J. M.; Mogne, Th. Le.; Vovelle, L. In *Metallized Plastics 2: Fundamental and Applied Aspects*; Mittal, K. L., Eds.; Plenum Press: New York, 1991; pp 219–231.
- (44) Inagaki, N.; Tasaka, S.; Masumoto, M. *Macromolecules* **1996**, *29*, 1642.
- (45) Bain, C. D.; Biebuyck, J.; Whitesides, G. M. *J. Am. Chem. Soc.* **1989**, *111*, 7155.
- (46) Whitesides, G. M.; Laibinis, P. E. *Langmuir* **1990**, *6*, 87.
- (47) Laibinis, P. E.; Whitesides, G. M.; Allara, D. L.; Tao, Y. T.; Parikh, A. N.; Nuzzo, R. G. *J. Am. Chem. Soc.* **1991**, *113*, 7152.
- (48) Steiner, U. B.; Caseri, W. R.; Suter, U. W. *Langmuir* **1993**, *9*, 877.
- (49) Steiner, U. B.; Caseri, W. R.; Suter, U. W.; Rehahn, M.; Schmitz, L. *Langmuir* **1993**, *9*, 3245.

MA982003Q